Reinvestigation of Dion-Jacobson Phases $CsCa_2Nb_2MO_9$ (M = Fe and Al)

Young-Sik Hong

*Department of Science Education, Seoul National University of Education, Seoul 137-742, Korea. *E-mail: njyshong@snue.ac.kr*
Received October 13, 2005

Dion-Jacobson phases $CsCa_2Nb_2FeO_9$ and $CsCa_2Nb_2AlO_9$ were reinvestigated by the Rietveld analysis of powder X-ray diffraction (XRD) method, scanning electron microscopy (SEM), and energy dispersive X-ray spectroscopy (EDS). These nominal compounds, previously known as the oxygen-deficient layered perovskites with the sequences of NbO_6-MO_4-NbO_6 in tripled slab, in fact, were mixed phases of n = 3 Dion-Jacobson phases and impurities such as Ca_2NbFeO_6 and $Ca_3Al_2O_6$. The difference of morphology and chemical in-homogeneity between Dion-Jacobson phases and impurities could be clearly identified by scanning electron microscopy with energy-dispersive X-ray spectroscopy. The chemical composition of $CsCa_2Nb_2FeO_9$ was calculated into $Cs_{0.59}Ca_{2.64}Nb_{2.92}Fe_{0.81}$ in small agglomerate crystals and $Cs_{0.95}Ca_{1.97}Nb_{3.08}Fe_{0.15}$ in long plate-like crystals.

Key Words : Oxide, Layered compound, Perovskite, Dion-Jacobson phase

Introduction

Since the discovery of layered perovskites such as Aurivillius and Ruddlesden-Popper phases, many layered perovskites based on $A_{n-1}B_nO_{3n+1}$ slabs have been described. In 1981, Dion *et al.* prepared new family of layered perovskites, $A'Ca_2Nb_3O_{10}$ (A' = K, Rb, Cs, and Tl).[1] These compounds also consist of perovskite-structured slabs $A_{n-1}B_nO_{3n+1}$, which are separated by large A' cations along one of the perovskite cubic directions. Subsequently, a series of compounds, $A'[Ca_2Na_{n-3}Nb_nO_{3n+1}]$ (A' = K, Rb, Cs and n = 3-7), were synthesized and named Dion-Jacobson phases.[2] Other related layered perovskites such as $A'LaNb_2O_7$ (A' = Li, Na, K, Rb, Cs, and NH_4), $A'BiNb_2O_7$ and $A'Pb_2Nb_3O_{10}$ (M = Rb and Cs), $KCa_2(Ca,Sr)_{n-3}Nb_3Ti_{n-3}O_{3n+1}$ (n = 4 and 5), and $K_{1-x}La_xCa_{2-x}Nb_3O_{10}$ were characterized.[3-6]

The diversity of cations that the perovskite structure can accommodate proves important when trying to introduce oxygen vacancies by doping with aliovalent cations. For example, Uma and Gopalakrishnan synthesized the new Dion-Jacobson phases with the formula $CsCa_2Nb_{3-x}M_xO_{10-x}$ (M = Fe and Al) and proposed their structures as oxygen-deficient compounds with the layer sequence of NbO_6-MO_4-NbO_6 in tripled slabs.[7] However, they just provided the index data of XRD patterns without any structural characterizations such as Rietveld analysis and/or electron diffraction patterns. Since 2-dimensional perovskites have the similar perovskite-structured units ABO_3 and/or $A_{n-1}B_nO_{3n+1}$, they may have similar unit cell parameters of *a* and *b*. It means that some of their Bragg reflections would likely overlap in 2- and 3-dimensional directions. This is why the observed intensities of layered perovskites as well as Bragg positions should be carefully characterized.

In this regard, this work readdresses $CsCa_2Nb_2FeO_9$ and $CsCa_2Nb_2AlO_9$, still misunderstood as oxygen-deficient Dion-Jacobson phases. Conclusively saying, these are not the oxygen-deficient phases but the mixed phases of 2-D layered perovskites and impurities.

Experimental Section

$CsCa_2Nb_2MO_9$ were prepared by the conventional solid-state reaction. The starting materials used were Cs_2CO_3, $CaCO_3$, Nb_2O_5, Fe_2O_3, and Al_2O_3 (Aldrich Chemicals, 99%). A 25 mole% excess of Cs_2CO_3 was used in the reactions to compensate for the volatilization of the Cs component at higher synthetic temperature. The reactants were ball-milled in ethanol for 12 h, and then the mixed powder was fired at 1423 K in air for 48 h in a covered Al_2O_3 crucible. The products were washed with distilled water to remove excess Cs component, and were dried in air. For comparison, the $CsCa_2Nb_3O_{10}$ was also prepared.

Powder X-ray diffraction (XRD, Philips X'pert MPD) data were recorded at room temperature using Bragg-Brentano geometry with CuK_a radiation. Step scans were performed over the angular range $10 < 2\theta/^o < 100$ with the step size of 0.02^o and the counting time of 10 second per step. The crystal structures were refined by the Rietveld method using the FULLPROF program.[8] The peak shape was described by a pseudo-Voigt function. The background level was defined by a polynomial function. For each diffraction pattern, the scale factor, the counter zero point, the peak asymmetry and the unit-cell dimensions were refined in addition to the atomic parameters.

The powder morphologies were examined using a scanning electron microscope (SEM, JEOL JSM-5310LV). An elemental analysis was carried out using the energy dispersive X-ray spectroscopy (EDS) attached in the SEM.

Results and Discussion

$CsCa_2Nb_2FeO_9$. The powder XRD pattern of $CsCa_2Nb_2FeO_9$ was indexed on a tetragonal cell with $a \sim 3.87$ Å and $c \sim 15.09$ Å. It shows that the peak positions and intensities of the obtained phase well correspond to the $CsCa_2Nb_2FeO_9$ known as oxygen-deficient phase in ref. 7, as listed in Table 1. To simplify the structural analysis, the crystal

Table 1. Comparison of powder XRD data for $CsCa_2Nb_2FeO_9$

	Ref. 7 (P4/mmm)		This work (P4/mmm)	
(h k l)	d_{obs}	I_{obs}	d_{obs}	I_{obs}
(1 0 0)	3.883	15	3.857	17
(0 0 4)	3.778	100	3.754	100
(1 0 2)	3.447	13	3.430	10
(1 0 3)	3.079	45	3.057	34
(0 0 5)	3.023	20	3.008	16
(1 1 0)	2.743	43	2.730	37
(0 0 6)	2.516	5	2.509	7
(1 1 4)	2.217	3	2.210	2
(0 0 7)	2.161	15	2.150	16
(1 0 6)	2.113	4	2.106	3
(2 0 0)	1.937	18	1.932	17

structure was supposed to the tetragonal cell with space group *P4/mmm*. First of all, the Nb^{5+} and Fe^{3+} cations were situated in the 2g (0, 0, ~0.28) and 1a (0, 0, 0) sites as in $CsLn_2Ti_2NbO_{10}$[9], resulting in the ordering sequence of NbO_6-FeO_4-NbO_6.[7] As shown in Figure 1(a), most of the observed XRD patterns of $CsCa_2Nb_2FeO_9$ were superimposed on the calculated Bragg reflections, but a careful inspection of individual reflections indicated that there were significant differences for the (100), (110), and (200) reflections. As a result, the refinement gave the abnormally high agreement factors of R_p = 49.8%, R_{wp} = 53.1%, and R_I = 39.3%. In the second place, the random sequence of $(Nb_{2/3}Fe_{1/3})O_{5.33}$-$(Nb_{2/3}Fe_{1/3})O_{5.33}$-$(Nb_{2/3}Fe_{1/3})O_{5.33}$ and the new-type ordering sequence of $(Nb_{1/2}Fe_{1/2})O_5$-NbO_6-$(Nb_{1/2}Fe_{1/2})O_5$ in the tripled perovskite slabs were adopted, but the agreement factors were not improved.

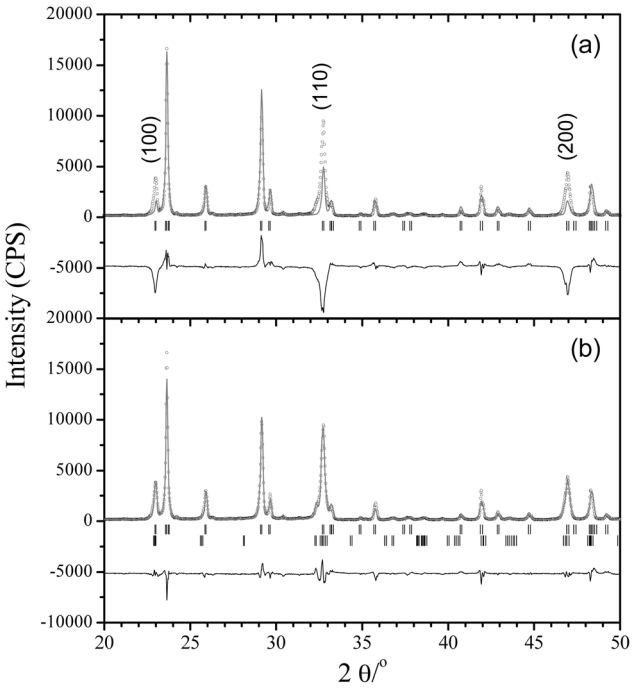

Figure 1. Selected observed, calculated, and difference powder XRD profiles of $CsCa_2Nb_2FeO_9$. (a) single-phase model and (b) two-phase model. Small bars indicate the positions of Bragg reflections for Dion-Jacobson phase (upper bars) and 3-dimensional perovskite (lower bars). The difference between the calculated and experimental patterns is plotted along the bottom.

The big difference between the observed and calculated intensities in Figure 1(a) indicates that the obtained product was not single-phase compound but mixture of 2- and 3-dimensional perovskites. From the JCPDS file, it was found that most of reflections of 3-dimensional Ca_2NbFeO_6 compound coincided with those of the obtained product.[10] Therfore, refinement was carried out using two compositions of $CsCa_2Nb_3O_{10}$ and Ca_2FeNbO_6 (space group $P2_1/n$), as shown in Figure 1(b). For Ca_2NbFeO_6, only the unit cell parameters were allowed to refine the profile. Then the agreement factors were significantly improved to R_p = 17.4%, R_{wp} = 22.5%, $R_{I(phase\ 1)}$ = 9.88% and $R_{I(phase\ 2)}$ = 3.51%. Although the agreements factors were still high, at least, it can be concluded that the obtained product was not a single-phase compound but the mixture of Dion-Jacobson phase and 3-dimensional perovskite.

To confirm the phase segregation, SEM and EDS analyses were used. Figure 2 shows the SEM photographs for $CsCa_2Nb_3O_{10}$ and nominal $CsCa_2Nb_2FeO_9$. The crystals of $CsCa_2Nb_3O_{10}$ consist of small plate-like ones of 1-4 μm. Meanwhile, the crystals of nominal $CsCa_2Nb_2FeO_9$ show two distinct morphologies, one is long plate-like crystals and the other is small agglomerate crystals of about 1-3 μm. Figure 3 shows the EDS results for the two different parts of nominal $CsCa_2Nb_2FeO_9$. It was found that the composition of part A and B were $Cs_{0.95}Ca_{1.97}Nb_{3.08}Fe_{0.15}$ and $Cs_{0.59}Ca_{2.64}Nb_{2.92}Fe_{0.81}$ (Table 2), respectively, result in significant chemical inhomogeneity with high and low iron contents. This means

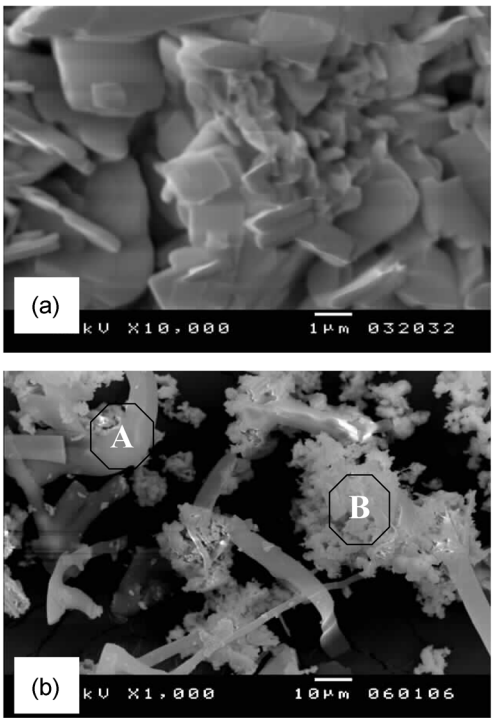

Figure 2. Scanning electron microphotographs of (a) $CsCa_2Nb_3O_{10}$ and (b) nominal $CsCa_2Nb_2FeO_9$.

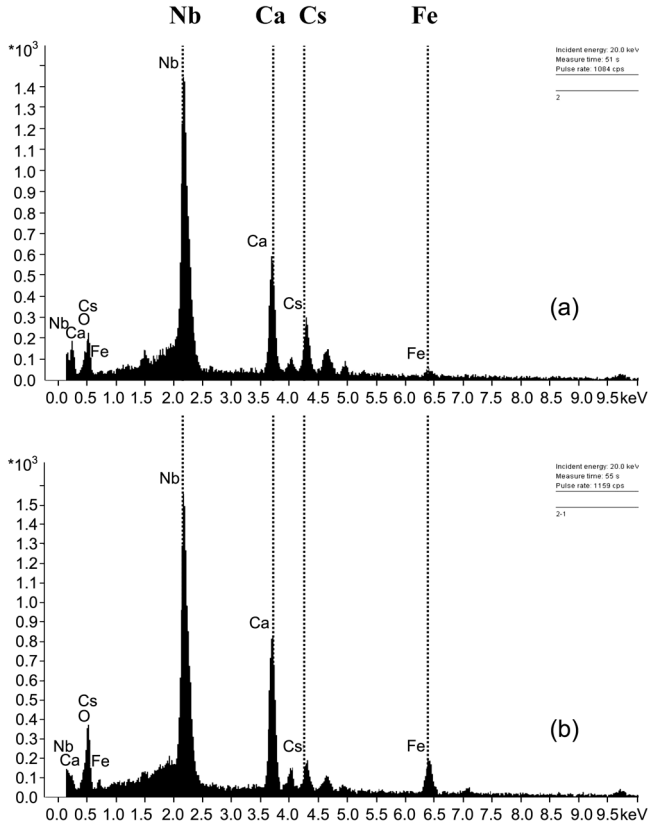

Figure 3. Energy dispersive X-ray emission spectra of (a) part A and (b) part B marked in Figure 2(b).

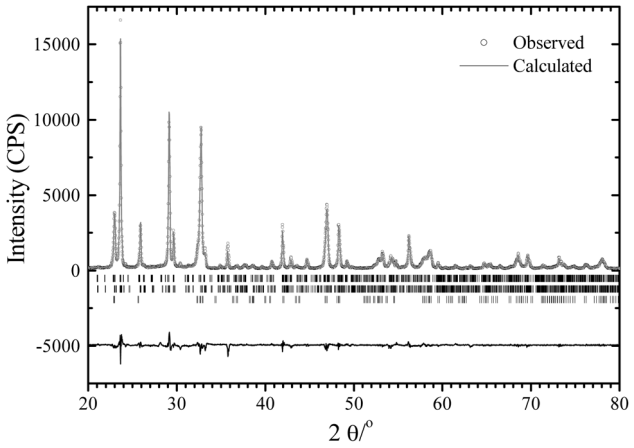

Figure 4. Selected observed, calculated, and difference powder XRD profiles of nominal $CsCa_2Nb_2FeO_9$, according to the three-phase model. Small bars indicate the positions of Bragg reflections for $Cs_{0.95}Ca_{1.97}Nb_{3.08}Fe_{0.15}O_{10.13}$ (upper bars), $CsCa_2Nb_3O_{10}$ (middle bars), and Ca_2NbFeO_6 (lower bars).

that the long plate-like crystals were iron-doped layered perovskite $CsCa_2Nb_{3-x}Fe_xO_{10-x}$ (x~0.15, phase 1). Meanwhile, the small agglomerate crystals were consisted of two phases of 2- and 3-dimensional perovskites, because the cesium cation is too large to occupy the A-site of 3-dimensional perovskite. Then, their compositions were simply supposed to $CsCa_2Nb_3O_{10}$ (phase 2) and Ca_2NbFeO_6 (phase 3).

One more point to note is the symmetry of calcium-containing phases 1 and 2. Actually, the symmetry of $CsCa_2Nb_3O_{10}$ in A-site are lowered from tetragonal to orthorhombic.[11] Finally, the refinement was carried out using the space group *Pnam* ($a = 2 \times c_p$, $b = 2 \times a_p$, and $c = 2 \times a_p$), where a_p and c_p are the unit cell parameters in a primitive tetragonal cell. Since it is difficult to determine the accurate positions of oxygen atom due to its smaller contribution to the structure factors, especially for the complex structure with many oxygen sites, the atomic positions for oxygens were fixed to those of $CsCa_2Nb_3O_{10}$.[11] Within the space group *Pnam* for phase 1 and 2, the unit cell parameters and preferred orientation factor were allowed to vary independently, as well as a phase fraction parameter. For the phase 1, the Nb/Fe occupation factors were fixed to the value obtained by elemental analysis. Then, the agreement factors are significantly improved to $R_p = 11.2\%$, $R_{wp} = 14.7\%$, and $R_{I(phase\ 1)} = 5.78\%$, $R_{I(phase\ 2)} = 5.98\%$, and $R_{I(phase\ 3)} = 2.46\%$. Figure 4 shows the selected observed, calculated, and difference powder XRD profiles of $CsCa_2Nb_2FeO_9$, according to the three-phase model. The unit cell parameters refined by space group *Pnam* are listed in Table 3. The percentages of each phase were refined to 23% (phase 1), 46% (phase 2), and 31% (phase 3), respectively. In the refinement, the preferred orientation factors for phases 1 and 2 were obtained using the March's function, $y = G2 + (1\text{-}G2) \times (G1 \times \cos\theta)^2 + (\sin\theta)^2/G1)^{-1.5}$, where G1 is a refinable parameter and θ is the acute angle between the scattering vector and the normal to the crystallites.[8] The G1 values obtained were 0.38(1) for phase 1, confirming the plately morphological feature in Figure 2.

$CsCa_2Nb_2AlO_9$. The powder XRD pattern of nominal $CsCa_2Nb_2AlO_9$ was not refined by a single-phase model, as shown in Figure 5(inset). Figure 6 shows the mixed morphologies consisted of rectangular plate-like and agglomerate crystals. The elemental analysis of nominal $CsCa_2Nb_2AlO_9$ indicated that the rectangular plate-like crystals (part A, $Cs_{0.76}Ca_{1.82}Nb_{2.56}Al_{0.52}$) contain lower contents of calcium and aluminum than small agglomerate crystals (part B, $Cs_{0.33}Ca_{3.08}Nb_{2.30}Al_{1.64}$). Therefore, the refinement was carried out using two-phase model, consisting of $CsCa_2Nb_3O_{10}$ and

Table 2. Elemental analysis of $CsCa_2Nb_3O_{10}$ and $CsCa_2Nb_2MO_9$

	Area	Cs	Ca	Nb	Fe	Al	Composition
$CsCa_2Nb_3O_{10}$		26.1(0.7)	17.0(0.8)	56.9(1.3)			$Cs_{0.98}Ca_{2.12}Nb_{3.06}$
$CsCa_2Nb_2FeO_9$	A	25.3(0.7)	15.8(0.4)	57.2(1.6)	1.7(0.5)		$Cs_{0.95}Ca_{1.97}Nb_{3.08}Fe_{0.15}$
	B	15.6(4.1)	21.1(0.3)	54.2(6.1)	9.1(1.8)		$Cs_{0.59}Ca_{2.64}Nb_{2.92}Fe_{0.81}$
$CsCa_2Nb_2AlO_9$	A	23.8(1.9)	17.1(0.8)	55.8(2.1)		3.3(0.9)	$Cs_{0.76}Ca_{1.82}Nb_{2.56}Al_{0.52}$
	B	10.3(2.8)	29.0(1.8)	50.3(5.1)		10.4(1.5)	$Cs_{0.33}Ca_{3.08}Nb_{2.30}Al_{1.64}$

Table 3. Refined unit cell parameters and weighted % of $CsCa_2Nb_2MO_9$

	Phase (composition)[a]	a (Å)	b (Å)	c (Å)	β(°)	Weighted %
M = Fe	1 ($Cs_{0.95}Ca_{1.97}Nb_{3.08}Fe_{0.15}$)	30.1577(8)	7.795(2)	7.769(3)		23
	2 ($CsCa_2Nb_3O_{10}$)	30.1663(9)	7.7432(4)	7.7325(3)		46
	3 (Ca_2NbFeO_6)	5.4431(6)	5.5412(5)	7.7511(6)	90.082(9)	31
M = Al	1 ($CsCa_2Nb_3O_{10}$)	30.262(2)	7.742(2)	7.750(2)		75
	2 ($Ca_3Al_2O_6$)	15.3059(9)				25

[a]These are not real compositions but used ones in the refinement.

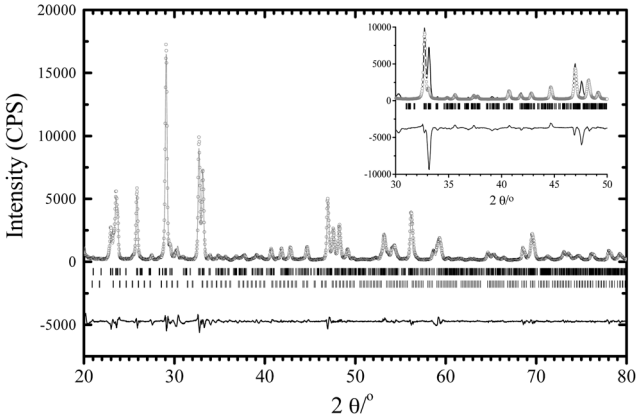

Figure 5. Selected observed, calculated, and difference powder XRD profiles of nominal $CsCa_2Nb_2AlO_9$, according to the two-phase model. Small bars indicate the positions of $CsCa_2Nb_3O_{10}$ (upper bars) and $Ca_3Al_2O_6$ (lower bars). The inset shows the refined profiles by single-phase model.

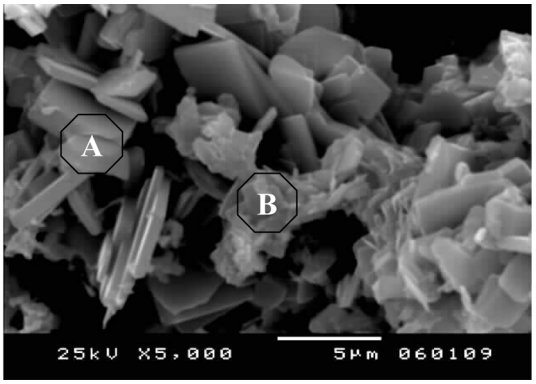

Figure 6. Scanning electron microphotographs of $CsCa_2Nb_2AlO_9$.

$Ca_3Al_2O_6$ (JCPDS No. 38-1429, space group *Pa3*). Then, the agreement factors were significantly improved from R_p = 19.3%, R_{wp} = 23.3%, and R_I = 10.9% for single-phase model to R_p = 11.4%, R_{wp} = 16.1%, $R_{I(phase\ 1)}$ = 3.81%, and $R_{I(phase\ 2)}$ = 2.69% for two-phase model. The lattice parameters refined by space group *Pnam* are listed in Table 3.

Interpretation of Organic Amine Intercalation. Uma and Gopalakrishnan reported that the intercalation of 0.6 mole of amine per formula unit of the host solid could be explained as the different acidity of the protons in $HCa_2Nb_2MO_9$. They suggested that there exist three kinds of protons such as NbO-H-ONb, NbO-H-OM, and MO-H-OM in the interlayer of $HCa_2Nb_2MO_9$. According to them, the protons in NbO-H-ONb and NbO-H-OM could react with organic amines since Nb^{5+}-O-H bond has stronger inductive effect and acidity than M^{3+}-O-H. However, this is not the reason. Actually, the refined percentages of layered perovskites were well consistent with the intercalated amine content, that is, 69% for nominal $CsCa_2Nb_2FeO_9$ and 75% for nominal $CsCa_2Nb_2AlO_9$ (Table 3). Therefore, the contents of intercalated organic amines nearly correspond to the mole fractions of synthesized layered perovskite compounds.

In conclusion, it was confirmed that nominal compounds $CsCa_2Nb_2FeO_9$ and $CsCa_2Nb_2AlO_9$ were not single-phase compound but mixed-phase of 2- and 3-dimensional perovskites. The impurities of each phase were mainly Ca_2NbFeO_6 and $Ca_3Al_2O_6$. Although it cannot be totally discard the possibility that these impurities are the reaction intermediates, the oxygen-deficient Dion-Jacobson phases could not be easily prepared by the conventional solid-state reaction. Nonetheless, many research groups have been wrongly citing the nominal compounds $CsCa_2Nb_2MO_9$ as new oxygen-deficient Dion-Jacobson phases in their publications. Recently, it was found that the Dion-Jacobson phases $CsLn_2Ti_2NbO_{10}$ (Ln = La, Pr, Nd, Sm) show the new-type B-cation arrangement of $(Ti_{1/2}Nb_{1/2})O_6$-TiO_6-$(Ti_{1/2}Nb_{1/2})O_6$.[9] In this regard, the synthesis of 2-dimensional perovskite compounds should be carefully characterized in view of the possibility of unwanted 3-dimenstional perovskite phase and new-type B cation arrangements.

References

1. Dion, M.; Ganne, M.; Tournoux, M. *Mater. Res. Bull.* **1981**, *16*, 1429.
2. Jacobson, A. J.; Johnson, J. W.; Lewandowski, J. T. *Inorg. Chem.* **1985**, *24*, 3727.
3. Gopalakrishnan, J.; Bhat, V.; Raveau, B. *Mater. Res. Bull.* **1987**, *22*, 413.
4. Subramanian, M. A.; Gopalakrishnan, J.; Sleight, A. W. *Mater. Res. Bull.* **1988**, *23*, 837.
5. Mohan Ram, R. A.; Clearfield, A. *J. Solid State Chem.* **1991**, *94*, 45.
6. Uma, S.; Gopalakrishnan, J. J. *Solid State Chem.* **1993**, *102*, 332.
7. Uma, S.; Gopalakrishnan, J. *Chem. Mater.* **1994**, *6*(7), 907.
8. Rodriguez-Carvajal, J. *Program Fullprof*, version 3.2; Laboratoire Leon Brillouin: January, 1997.
9. Hong, Y.-S.; Kim, S.-J.; Kim, S.-J.; Choy, J.-H. *J. Mater. Chem.* **2000**, *10*, 1209.
10. Chakhmouradian, A. R.; Mitchell, R. H. *J. Solid State Chem.* **1998**, *138*, 272.
11. Dion, M.; Ganne, M.; Tournoux, M.; Ravez, J. *Revue de Chimie Minérale* **1984**, *21*, 92.
12. Fair, G.; Shemkunas, M.; Petuskey, W. T.; Sambasivan, S. J. *Euro. Ceram. Soc.* **1999**, *19*, 2437.